Numerical Algorithms for Turbulent Mixing Simulations

O. Schilling

University of California, Lawrence Livermore National Laboratory,
Livermore, California, 94550

The desirable features of algorithms for the direct, implicit large-eddy, and large-eddy numerical simulation of compressible turbulent mixing are discussed. Issues specific to turbulence and mixing induced by interfacial instabilities are briefly reviewed. A high-resolution, Eulerian numerical algorithm for compressible turbulent mixing simulations currently in use at the Lawrence Livermore National Laboratory (LLNL) is described–the weighted essentially non-oscillatory (WENO) method. The method is applied to the two-dimensional reshocked Richtmyer-Meshkov instability using third-, fifth-, and ninth-order reconstruction, and the dependence of quantities on both the grid resolution and order of spatial flux reconstruction is investigated. It is shown that certain large-scale quantities exhibit little sensitivity to both the resolution and order prior to reshock, but exhibit much greater sensitivity following reshock. The dependence of various quantities determined by the entire range of resolved scales (such as energy spectra and mixing characteristics) on the resolution and order is also discussed. It is concluded that lower-order reconstruction and lower resolution result in excessively large numerical dissipation. The implications of these results for simulating experiments and assessing turbulent transport and mixing models are briefly discussed.

Introduction

The numerical simulation of turbulent mixing induced by hydrodynamic interfacial (i.e., Rayleigh-Taylor and Richtmyer-Meshkov) instabilities presents a number of challenges with respect to both physics and numerical algorithms. These challenges must be addressed in order to perform realistic simulations of experiments conducted in parameter regimes of physical interest, as well as to generate datasets that can be used for turbulent transport and mixing model assessment and development. Such numerical simulations have a role in diverse applications including astrophysics (particularly supernovae), inertial confinement fusion, and fundamental studies of buoyancy- and acceleration-driven, inhomogeneous turbulent flows. To a large extent, the flow physics of interest dictates the characteristics that must be satisfied by the numerical method used. In addition, it is essential to understand how the numerical method used affects the flow field: for numerical methods designed to solve the non-dissipative compressible fluid dynamics equations (i.e., the Euler equations), this typically entails grid convergence studies and various verification and validation studies involving comparisons to analytical or semi-analytical solutions, or to available experimental data.

The organization of this contribution is as follows. First, the physical and numerical issues pertinent to simulating compressible turbulent mixing will be succinctly reviewed to suggest a set of desirable features that a numerical algorithm should possess in order to accurately simulate turbulent mixing. Second, numerical methods and approaches used to simulate such flows will be briefly reviewed, together with more recent approaches that have promise. Third, the weighted essentially non-oscillatory (WENO) method currently in use at LLNL will be briefly described. Fourth, the WENO method is applied to the two-dimensional Richtmyer-Meshkov instability with reshock using different grid resolutions and orders of spatial reconstruction; several quantities characterizing the mixing and turbulent properties of the flow are compared from these simulations. Finally, the results of the numerical experiments are summarized and conclusions are drawn.

Physical, Numerical, and Theoretical Considerations Regarding the Simulation of Compressible Turbulent Mixing

When taken together, the physical and numerical considerations that arise in simulating compressible turbulent mixing limit the possible candidate numerical algorithms/methods that should be used for turbulent mixing simulations.

Physical Considerations

With regard to the flow physics, the issues that must be considered include the following. *First*, at very large Reynolds numbers, the range of spatial scales that must be resolved is too large to allow direct numerical simulation using molecular dissipation and diffusion coefficients that are realistic. *Second*, in the presence of shocks and material discontinuities, it is not strictly possible to directly simulate the flow due to the inability to fully resolve shocks. *Third*, these flows are initiated from small-scale initial fields that are computationally expensive to resolve. *Fourth*, these flows are typically transitional, i.e., develop from quiescent initial conditions through a linear and nonlinear growth stage into a fully turbulent state. *Fifth*, the anisotropic flow consists of vortical structures of different sizes resulting from a complex interaction between buoyancy and/or baroclinic and shear effects. These issues also complicate the development of appropriate models for representing transport and mixing, i.e., both subgrid-scale (for large-eddy simulation with explicit subgrid modeling) and Reynolds-averaged Navier-Stokes (RANS) models.

Numerical Considerations

With regard to the numerical algorithms, the issues that must be considered include the following. *First*, the numerical method must be able to represent propagating shocks and associated waves, as well as resolve any material discontinuities. *Second*, the numerical algorithm must be conservative and computationally robust over a wide range of simulation parameters. *Third*, the algorithm must be sufficiently accurate in both space and time to resolve all of the scales present in the flow over the simulation time with minimal dissipative and dispersive error. *Fourth*, the multi-component character of the mixing fluids must be approximated mathematically and discretized numerically (there is no unique description of a multi-component or multi-species flow).

Theoretical Considerations

A number of theoretical considerations regarding shocks and, more generally, discontinuities and hyperbolic partial differential equations are relevant to the present discussion. For example, it is well-known that the convergence rate of an nth-order finite-difference approximation to the solution of hyperbolic partial differential equations may give worse than nth-order convergence if the $(n+1)$st derivatives of the solution are not piecewise continuous (Orszag and Jayne, 1974). Furthermore, *when the solution is not globally smooth, a fixed stencil interpolation of second or higher order is necessarily oscillatory near a discontinuity*. Such oscillations can be suppressed using filtering (Majda et al., 1978; Mock and Lax, 1978; Engquist et al., 1989; Vandeven, 1991; Don, 1994; Gottlieb and Hesthaven, 2001). The degradation of the solution downstream from the shock is due to the propagation of errors with outgoing characteristics, as shown numerically using the ENO method (Donat and Osher, 1990; Donat, 1994). For a *linear* problem, high-order (or high-resolution) methods give high-order results for moments, so that accurate pointwise values can be reconstructed in smooth regions. For a *nonlinear* problem, the accuracy is reduced to first-order upon shock passage (Majda and Osher, 1977; Engquist and Sjögreen, 1998). It should be noted, however, that methods have been developed in an attempt to mollify these errors: a matched asymptotic expansion analysis was used to modify the artificial viscosity in one- and two-dimensional shock-capturing schemes for hyperbolic equations with a source term to raise the order of accuracy from first-order downstream of shocks to second-order (Kreiss et al., 2001). This analysis was extended to the case of time-dependent shock calculations with a modified equation containing a matrix-valued viscosity coefficient (Siklosi and Kreiss, 2003). The issue of shock-induced numerical error is common to *all* numerical methods, and is not addressed further in the present work.

Brief Review of Numerical Methods for Simulating Compressible Turbulent Mixing

The summary of numerical methods below focuses on methods that have been applied to simulations of mixing induced by shocks. Each of these methods have relative advantages and disadvantages. The review given here is not exhaustive and, in particular, omits a description of adaptive mesh refinement (AMR), which is discussed elsewhere in these Proceedings (Lomov et al., 2005).

Direct Numerical, Implicit Large-Eddy, and Large-Eddy Simulation

Various numerical methods and approaches for simulating compressible turbulent mixing are briefly summarized here. Broadly, these methods can be categorized as direct numerical simulations (DNS), implicit large-eddy simulations (ILES), and large-eddy simulations (LES).

In a *direct numerical simulation (DNS)*, molecular dissipation and diffusion terms are explicitly included, and all spatio-temporal scales are resolved, by definition (Pope, 2000). In principle, if the equations solved adequately describe the flow of interest, DNS provides the most physically accurate description of the flow dynamics. No modeling of terms in the equations is required. In practice, DNS is limited to Reynolds numbers, Schmidt numbers, and other parameters that are well below (or above) the values that are relevant to flows of physical interest. The resolution requirements for DNS of turbulent

mixing and of reacting flows are much more stringent than for homogeneous turbulence. DNS is limited to mixing induced by very weak shocks.

In a *monotone-integrated large-eddy simulation (MILES) or implicit large-eddy simulation (ILES)*, the non-dissipative fluid dynamics equations are solved using a shock-capturing method with the fields regarded as implicitly filtered by the underlying numerical algorithm (e.g., a top-hat filter in a finite-volume method), and with an implicit subgrid-scale model provided by the intrinsic numerical dissipation arising from discretization errors or the nonlinear flux-limiters (Boris et al., 1992; Garnier et al., 1999; Margolin and Rider, 2002, 2005; Drikakis, 2002, 2003; Grinstein et al., 2005). An obvious question that arises is whether this intrinsic dissipation is an adequate representation of physical dissipation, i.e., what is the relationship between the implicit subgrid model and an explicit one? This question has been partially addressed by analyzing the discretization error for a particular finite-volume shock-capturing method using the modified equation method and showing that this error can be cast in the form of a conventional artificial viscosity (Margolin and Rider, 2005). Approximate and direct deconvolution methods (Adams and Stolz, 2002; Stolz and Adams, 2003) have also been applied to shock-turbulence interaction.

In a *large-eddy simulation (LES)*, the filtered fluid dynamics equations are solved, with unclosed subgrid-scale terms arising from the filtering modeled using explicit subgrid models (Pope, 2000; Sagaut, 2002). LES of turbulent mixing driven by buoyancy or shocks encounters several important difficulties. Aside from the conceptual issues of what the large-eddy equations actually mean, additional conceptual issues relating to non-periodic boundaries and complex flow geometries, flow transients (shocks and material discontinuities), and accounting for the baroclinic and multi-species diffusion effects that drive the turbulence and mixing, arise. In most LES formulations, it is not possible to define Reynolds, Schmidt, and other characteristic parameters of the flow. The filtered structure function model implemented in a second-order, central finite-volume method with a modified, local Jameson artificial viscosity has been used in LES of shock-turbulence interaction (Ducros et al., 1999). LES of shock/homogeneous turbulence interaction were performed with the Smagorinsky model, the mixed model, the dynamic Smagorinsky model, and the dynamic mixed model (Garnier et al., 2002a). LES of shock/boundary layer interaction were performed with the mixed-scale model (Sagaut, 2001), a nonlinear fifth-order WENO filter, a fourth-order central difference scheme, and a third-order TVD Runge-Kutta time-evolution scheme (Garnier et al., 2002b). These applications do not, however, entail fluid mixing.

Filtered Spectral, Reconstruction-Evolution, and Compact Methods

Filtered spectral and spectral multi-domain methods were primarily developed for simulations of supersonic turbulent combustion (Don and Quillen, 1995; Don et al., 2005). Such methods employ high-order filtering to reduce or eliminate Gibbs oscillations in spectral simulations containing propagating shocks and material discontinuities. Thus, excessively dissipative upwinding is avoided, but at the expense of explicit filtering (which acts dissipatively) to mitigate oscillations that would otherwise contaminate the flow field and violate physical constraints such as mass fractions bounded between zero and unity. Moreover, *global filtering introduces dissipation*

everywhere in the flow field. Local, adaptive filtering addresses this, however is not robust for complex, multi-dimensional flows. While filtered spectral methods have shown great promise for flows with moderate strength shocks, they are not generally robust for flows initiated by large Mach number shocks.

Reconstruction-evolution or *shock-capturing methods* (Laney, 1998; LeVeque, 2002) are the methods traditionally used to simulate compressible turbulent mixing. These upwind methods include the Godunov and higher-order Godunov methods, the Van Leer method, the piecewise-parabolic method (PPM), essentially non-oscillatory (ENO) methods, and weighted essentially non-oscillatory (WENO) methods. Reconstruction-evolution methods are based on: (1) a spatial reconstruction of the solution $\varphi(x,t_n)$ using a reconstruction algorithm, which may entail solution averaging and limiting, and; (2) evolution of the solution from t_n to t_{n+1} using wave- or characteristic-based methods. Such methods are also generically known as Godunov, MUSCL, and flux-difference splitting methods. These methods treat the flux using either a Riemann solver or by flux-splitting. Many modern reconstruction-evolution methods reconstruct either the numerical flux at cell edges in the pth characteristic field or the conserved variables pointwise at the cell edges $x_{i\pm1/2}$. These methods are robust and can be applied to very large Mach number shocks. However, their nonlinear implicit dissipation mechanisms require very high spatial resolutions to minimize numerical diffusion.

Central and upwind compact finite-difference and finite-volume methods are adaptations of traditional compact finite-difference and finite-volume schemes (Deng and Zhang, 2000; Wang & Huang 2002; Sengupta et al., 2004, 2005; Broeckhoven et al., 2004). These more recently developed methods are also robust, but are also dissipative and have not been applied to multi-dimensional flows.

Hybrid Methods

The recognition that many multi-scale flows contain regions with different flow dynamics and therefore, different numerical requirements, has engendered the development of hybrid algorithms, in which the advantageous features of each constituent algorithm are applied to different flow regions or directions. These hybrid methods typically combine (formally) high-order/high-resolution upwind and non-upwind algorithms. Recently developed hybrid methods include a spectral/compact finite-difference method (Cook and Dimotakis, 2001), a hybrid compact-WENO method (Pirozzoli, 2002; Ren et al., 2003), an optimized WENO method (Ponziani et al., 2003), a hybrid tuned central-difference/WENO method (Hill and Pullin, 2004), a WENO/central-difference method (Schilling and Latini, 2004), and a WENO/spectral multi-domain method (Don, 2005). An artificial hyperviscosity shock-capturing method (Cook and Cabot, 2005) is further described elsewhere in these Proceedings (Cook, 2005).

Application of the Weighted Essentially Non-Oscillatory (WENO) Method to Two-Dimensional Richtmyer-Meshkov Instability-Generated Flow

Presented here are selected results from a comprehensive investigation of mixing in two-dimensional Richtmyer-Meshkov instability with reshock (Schilling and Latini, 2005a). These can be regarded as numerical experiments indirectly investigating the dissipation properties of the WENO method.

Summary of the WENO Method

The present implementation of the flux-averaged WENO method uses local Lax-Friedrichs flux-splitting and a characteristic decomposition of the variables and fluxes (see Schilling and Latini, 2004 and references therein). At a given timestep, the numerical algorithm can be summarized as follows:

(1) compute the average state $\overline{\varphi}^{\alpha}$ at (i+1/2,j,k) using a Roe average;

(2) evaluate the left and right eigenvector matrices $\mathbf{L}(\overline{\varphi})$ and $\mathbf{R}(\overline{\varphi})$, and the eigenvalues of the Jacobian matrix at the average state;

(3) for every stencil, project the conservative fields and the fluxes onto the local characteristic directions using the left eigenvector matrix ($2r$ - 1 is the formal order of accuracy), $\varphi^{\alpha(ch)}_{m,j,k} = L(\overline{\varphi})\varphi^{\alpha}_{m,j,k}$ and $\hat{F}^{\alpha(ch)}_{m,j,k} = L(\overline{\varphi})F^{\alpha}_{m,j,k}$ with $m \in [i\text{-}r\text{+}1, i\text{+}r]$;

(4) evaluate the left and right characteristic fluxes $\hat{F}^{\alpha(ch)\pm}_{m,j,k}$ pointwise using local or global Lax-Friedrichs flux-splitting;

(5) reconstruct the numerical characteristic flux functions $\hat{F}^{\alpha(ch)\pm}_{m,j,k}$ from the pointwise values $\hat{F}^{\alpha}_{m,j,k}$ using the WENO method;

(6) compute the numerical flux function in physical space by projecting back using the right eigenvector matrix $\hat{F}^{\alpha}_{i+1/2,j,k} = R(\overline{\varphi})(\hat{F}^{\alpha,+}_{i+1/2,j,k} + \hat{F}^{\alpha,-}_{i+1/2,j,k})$

(7) obtain the fluxes in the y- and z-directions (i,j+1/2,k) and (i,j,k+1/2) accordingly, and;

(8) advance the solution one timestep using the third-order TVD Runge-Kutta scheme, and compute a new timestep based on the CFL criterion.

In the present parallel code, the one-, two-, or three-dimensional Euler equations can be solved, together with the mass fraction evolution equation.

Two-Dimensional Richtmyer-Meshkov Instability-Generated Flow with Reshock

The WENO method using a third-order total-variation diminishing Runge-Kutta time-evolution scheme is applied here to the single-mode Richtmyer-Meshkov instability with reshock in two spatial dimensions. The initial conditions and computational domain for the simulations are modeled after the Collins and Jacobs (2002) single-mode, Mach 1.21 air(acetone)/SF_6 shock tube experiment. The boundary conditions were: (1) periodic in the spanwise direction corresponding to the cross-section of the test section; (2) outflow at the entrance of the test section in the streamwise direction, and; (3) reflecting at the end wall of the test section in the streamwise direction. Simulations were performed using the third-, fifth-, and ninth-order WENO method with spatial resolutions corresponding to a uniform grid with 128, 256, and 512 points per initial perturbation wavelength (coarse, medium, and fine grids, respectively). The perturbation wavelength and amplitude were λ = 5.93 cm and a_0 = 0.2 cm, respectively. The computational domain consisted of only the test section of square cross-section 8.9 cm and length 75 cm. To specify a single value of the adiabatic exponent, a mixture of 50% air(acetone) and 50% SF_6 by volume was assumed, yielding $\gamma = 1.24815$.

As shown in Fig. 1, the perturbation amplitude $a(t)$ from the simulation is in generally very good agreement with the experimental data from Collins and Jacobs (2002) prior to

reshock; following reshock, the discrepancy is due to the influence of the rarefaction wave present in the experiment, but not in the simulation. The amplitude is defined as half of the mixing layer width $h(t)$, which is numerically determined by a 1-99% criterion in the mass fraction.

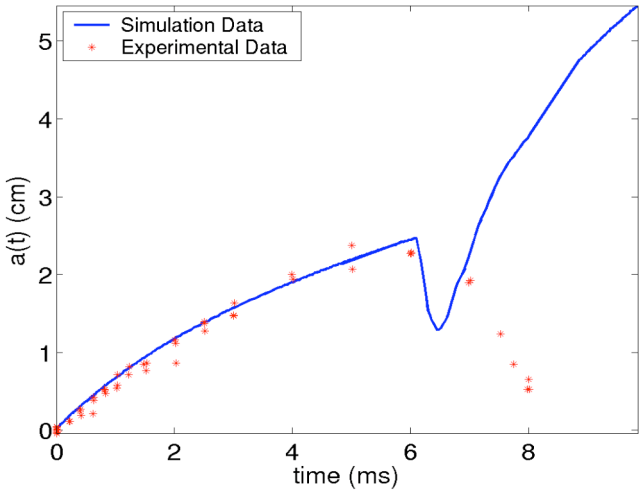

Figure 1. Perturbation amplitude $a(t)$ from the fifth-order WENO simulation on the medium resolution grid compared with the experimental data points.

Sensitivity of Quantities to the Order of Reconstruction and Grid Resolution

The sensitivity of various quantities to the formal order of flux reconstruction and to the grid resolution is investigated here. Figure 2 shows the mixing layer widths obtained using different orders and grid resolutions. With the exception of the third-order result on the coarse grid, the widths from the remaining simulations are in generally good agreement prior to reshock at ~ 6.5 ms; the widths are also in reasonable agreement for a short time following reshock. However, as the flow continues to develop after the reflected shock has moved away from the evolving layer, an increasingly large difference is observed among the widths. The widths from the ninth-order simulations are the largest and also grow fastest. The third-order widths differ significantly among the grid resolutions. The effects of wave interactions with the mixing layer are damped in the third-order results, but are present in the fifth- and ninth-order widths. Prior to reshock, all of the widths are larger than the ninth-order, fine grid width, and are within < 10% of one another. Following reshock, the widths are smaller than the ninth-order, fine grid width, consistent with the larger numerical dissipation in the lower-order, coarser grid simulations during the quasi-decay phase. The ninth-order widths appear to be nearly converged, even to late times.

Figure 3 shows an example of a quantity characterizing the global mixing properties, defined as follows. Suppose that the two fluids undergo a fast kinetic reaction, so that in terms of the mole fraction X the amount of product produced is $X_p(x,y,t) = X/X_s$ for $X \leq X_s$ and $X_p(x,y,t) = (1 - X)/(1 - X_s)$ for $X > X_s$ with $X_s = 1/2$ (representing equal mole fractions of the "reactants") (Koochesfahani and Dimotakis, 1986). Then the profile of the

averaged product mole fraction $\langle X_p \rangle(x,t) \in [0,1]$ provides information on how well mixed the two reactants are (angle brackets denote an average over the periodic y-direction). Then the total chemical product is $P_t(t) = \int_{a_s}^{a_b} \langle X_p \rangle dx$, where a_b and a_s are the bubble and spike amplitudes, respectively. Before reshock, P_t increases, indicating an increase in mixing. During reshock, the mixing layer is compressed, inducing additional mixing as measured by P_t. Following reshock, P_t increases rapidly, indicating significantly increased mixing. It is apparent that P_t is quite sensitive to the order and grid resolution.

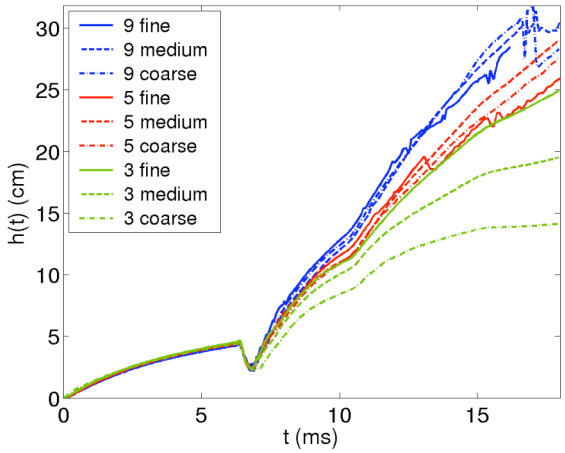

Figure 2. Comparison of the mixing layer width obtained from the third-, fifth-, and ninth-order WENO simulation on the fine, medium, and coarse grids.

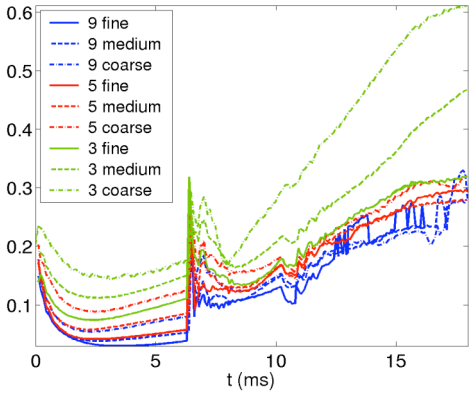

Figure 3. Time-evolution of the production fraction P_t obtained from the third-, fifth-, and ninth-order WENO simulation on the fine, medium, and coarse grids.

Figure 4 shows the one-dimensional turbulent kinetic energy, turbulent enstrophy, and density variance spectra obtained from the simulations with different orders and grid

resolutions at three different times (before and after reshock, and at late time). The turbulent kinetic energy spectrum is the least sensitive to the order and resolution. The large-scale (small k) kinetic energy spectra are in good agreement among the simulations, with most of the differences appearing in the intermediate scales. The turbulent enstrophy spectrum is the most sensitive to the order and resolution. As in the case of the turbulent kinetic energy spectrum, reshock primarily amplifies the turbulent enstrophy spectrum but does not change its shape. The spectra differ both in the large and smaller scales, with a very wide spread among the results obtained using different reconstruction orders and resolutions. The third- and fifth-order spectra are highly damped and decay rapidly with increasing wavenumber. The higher order, higher resolution simulations capture more small-scale vortical structure than the lower order, lower resolution simulations. The behavior of the density variance spectrum is qualitatively similar to that of the kinetic energy spectrum, and clearly shows that the spectra computed from the less dissipative algorithms extend further in wavenumber before dissipation begins to dominate.

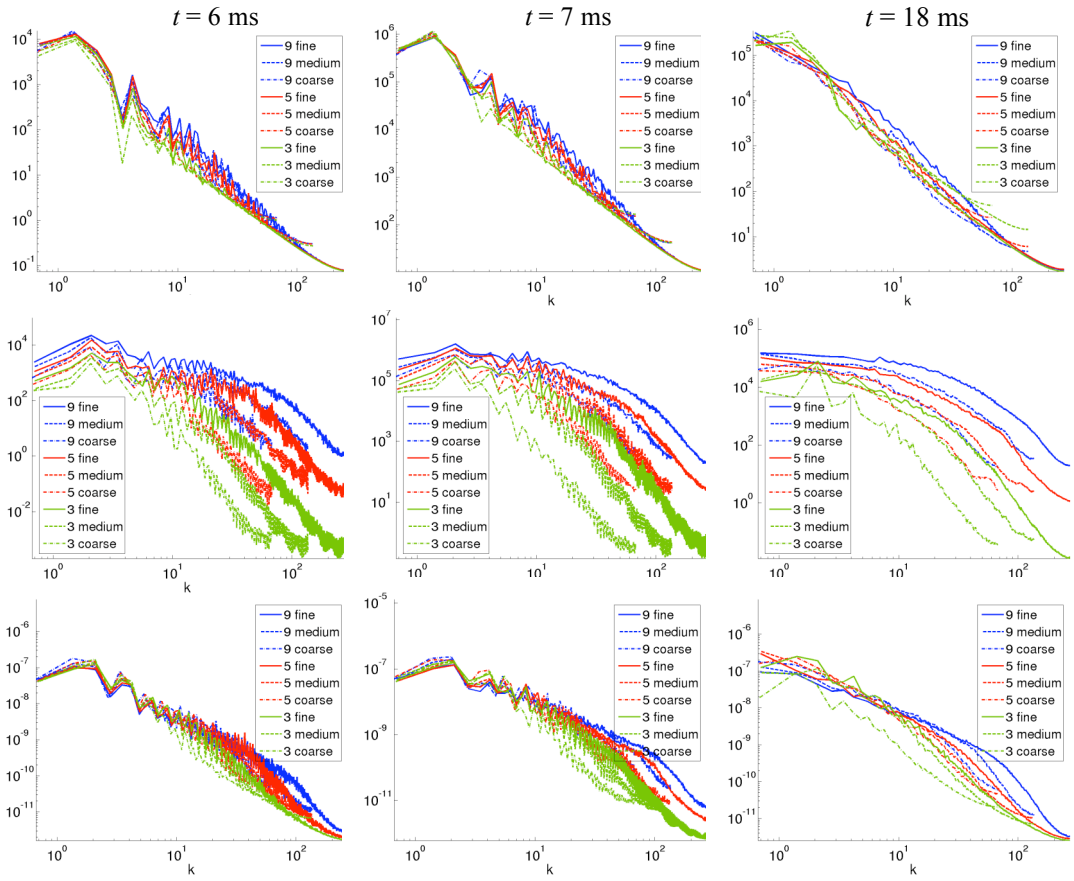

Figure 4. Turbulent kinetic energy (top row), turbulent enstrophy (middle row), and density variance (bottom row) spectra obtained from the third-, fifth-, and ninth-order WENO simulation on the fine, medium, and coarse grids.

Figures 5 and 6 show a comparison of the density field obtained from the third-, fifth- and ninth-order WENO simulations on the coarse, medium, and fine resolution grids at t = 6, 7, and 18 ms. Prior to reshock at t = 6 ms, the interface separating the gases is

highly diffused in the third-order simulations, which suppresses the roll-up of the interface and inhibits the formation of small-scale structure within the roll-ups. The ninth-order simulations show the most structure, particularly inside the roll-ups. Following reshock at $t = 7$ ms, the ninth-order, medium and fine grid simulations begin to show symmetry breaking, while the third- and fifth-order simulations continue to preserve symmetry. Many more fine-scale structures appear in the ninth-order simulations at all resolutions, compared to the fifth- and third-order simulations. The differences among these simulations are even more pronounced at late time, $t = 18$ ms, when the flow is in a quasi-decay phase (i.e., decaying but weakly influenced by waves). The third-order simulations continue to preserve symmetry, with large-scale structures dominating the flow. The coarse grid density shows a large degree of damping due to numerical dissipation. The ninth-order simulations exhibit the most asymmetry, disorder, and fine-scale structure qualitatively similar to that observed in shock tube experiments.

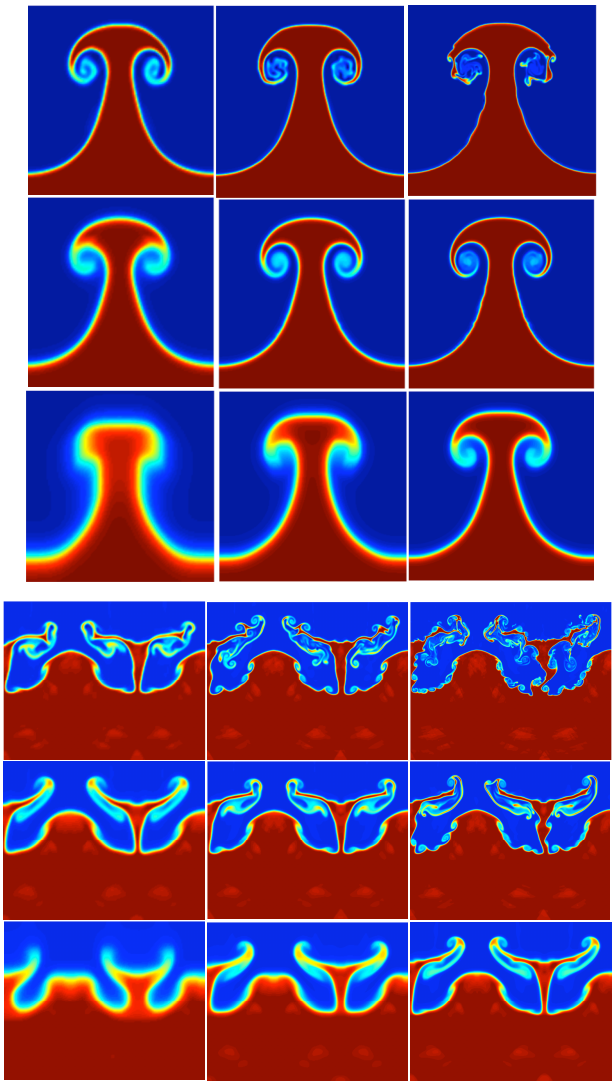

Figure 5. Comparison of the density field at time $t = 6$ ms (upper panel) and $t = 7$ ms (lower panel) obtained from the ninth- (top row), fifth- (middle row), and third-order

(bottom row) WENO simulations on the coarse (left column), medium (middle column), and fine (right column) grids.

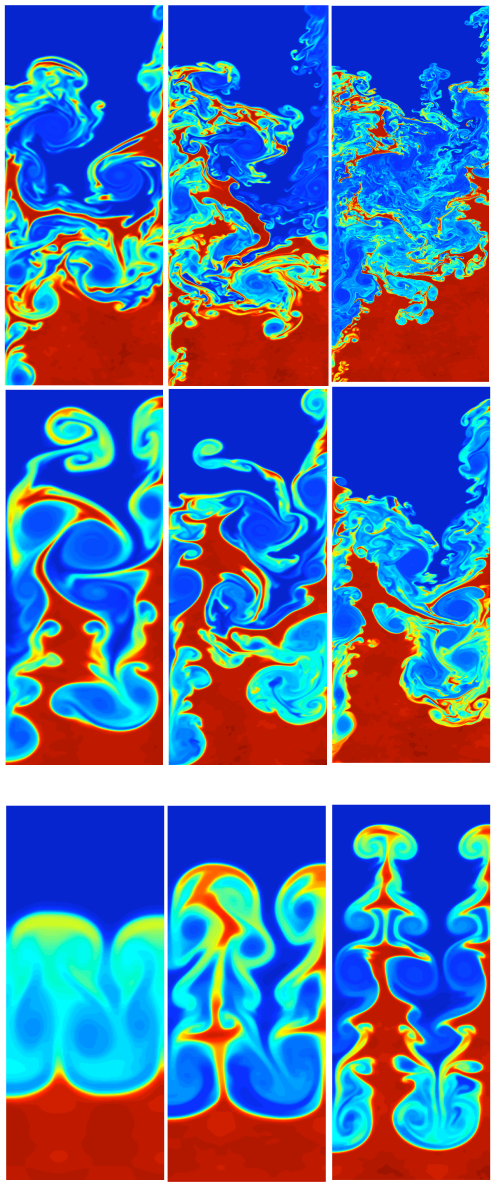

Figure 6. Comparison of the density field at time t =18 ms obtained from the ninth- (top row), fifth- (middle row), and third-order (bottom row) WENO simulations on the coarse (left column), medium (middle column), and fine (right column) grids.

Summary and Implications of the Results

The present investigation compared the results obtained from WENO shock-capturing simulations of the two-dimensional Richtmyer-Meshkov instability with reshock using different orders of flux reconstruction and grid resolution. The simulations were otherwise identical in all other respects. This systematic study quantitatively and qualitatively showed that lower order reconstruction and grid resolution yield both large- and smaller scale quantities that are strongly affected by the intrinsic numerical

dissipation present in the algorithm; this is particularly true at late times, when the flow is in a quasi-decaying state. For example, at late times, the mixing layer amplitudes differ considerably among the simulations with different orders and resolutions, with the ninth-order results showing evidence of convergence. Quantities characteristic of the mixing (e.g., production fractions) and of the distribution of energy fluctuations in various fields (velocity, vorticity, and density) also showed considerable differences as a function of order and resolution. Consequently, numerical dissipation in low-order simulations strongly damps fluctuations that affect *all* scales of the flow, and therefore, has significant implications for simulating turbulent mixing flows driven by baroclinic effects that affect the evolution of the vorticity field. While the dynamics of the flow evolution are expected to differ in three dimensions, the present study affords higher resolution per initial perturbation wavelength than is feasible in three dimensions. In addition, the numerical effects can be investigated in the absence of the effects of vortex stretching present in three-dimensional flow. It is expected that vortex stretching significantly affects mixing in three dimensions (Schilling and Latini, 2005b).

The results of this study also strongly suggest that higher-order methods must be used for LES with explicit subgrid-scale modeling, as the statistical effects represented by such models on the larger scale evolution will be significantly affected by the intrinsic numerical dissipation in the underlying hydrodynamic algorithm. This also has consequences for *a priori* turbulence model assessment using data obtained from high-resolution MILES or ILES. This study also shows that, in general, numerical 'convergence' must be assessed with respect to a range of quantities representative of the flow physics at all spatial scales.

Conclusions

The numerical experiments presented and discussed here suggest that higher order WENO methods (and hybridizations thereof) have great promise for the numerical simulation of compressible turbulent mixing induced by shocks. While all numerical methods are subject to $O(1)$ errors as a consequence of the passage of a shock through the domain, it is clear that early and late-time quantities are highly sensitive to the formal (or design) order of accuracy of the spatial discretization of the semi-discrete evolution equations. These conclusions are also consistent with the results of three-dimensional, fifth-, ninth-, and eleventh-order WENO simulations of the Vetter and Sturtevant (1995) Mach 1.5 air/SF_6 shock tube experiments (Schilling and Latini, 2005b).

Acknowledgements

I would like to thank my collaborators Marco Latini of Applied and Computational Mathematics at the California Institute of Technology and Dr. Wai-Sun Don of the Division of Applied Mathematics at Brown University. This work was performed under the auspices of the U.S. Department of Energy by the University of California Lawrence Livermore National Laboratory under Contract No. W-7405-Eng-48.

References

Adams, N. A., and Stolz, S. "A Subgrid-Scale Deconvolution Approach for Shock Capturing," *J. Comp. Phys.* **178**, 391–426 (2002).

Boris, J. P., Grinstein, F. F., Oran, E. S., and Kolbe, R. L., "New insights into large eddy simulation," *Fluid Dyn. Res.* **10**, 199–228 (1992).

Broeckhoven, T., Smirnov, S., Ramboer, J., and Lacor, C., "Finite Volume Formulation of Compact Upwind and Central Schemes with Artificial Selective Dissipation," *J. Sci. Comp.* **21**, 341–367 (2004).

Collins, B. D., and Jacobs, J. W., "PLIF flow visualization and measurements of the Richtmyer-Meshkov instability of an air/SF_6 interface," *J. Fluid Mech.* **464**, 113–136 (2002).

Cook, A. W., "Comparison of Modern Methods for Shock Hydrodynamics," Proceedings of the Five-Laboratory Conference on Computational Mathematics, Vienna, Austria, 19–23 June 2005 (2005).

Cook, A. W., and Cabot, W. H., "Hyperviscosity for shock-turbulence interactions," *J. Comp. Phys.* **203**, 379–385 (2005).

Cook, A. W., and Dimotakis, P. E., "Transition stages of Rayleigh-Taylor instability between miscible fluids," *J. Fluid Mech.* **443**, 69–99 (2001).

Deng, X., and Zhang, H., "Developing High-Order Weighted Compact Nonlinear Schemes," *J. Comp. Phys.* **165**, 22–44 (2000).

Don, W. S., "Numerical Study of Pseudospectral Methods in Shock Wave Applications," *J. Comp. Phys.* **110**, 103–111 (1994).

Don, W.-S., Brown University, Providence, Rhode Island, private communication (2005).

Don, W.-S., Gottlieb, D., and Jung, J.-H., "A multidomain spectral method for supersonic reactive flows," *J. Comp. Phys.* (2005).

Don, W. S., and Quillen, C. B., "Numerical Simulation of Shock-Cylinder Interactions. I: Resolution," *J. Comp. Phys.* **122**, 244–265 (1995).

Donat, R., "Studies on Error Propagation for Certain Nonlinear Approximations to Hyperbolic Equations: Discontinuities in Derivatives," *SIAM J. Num. Anal.* **31**, 655–679 (1994).

Donat, R., and Osher, S., "Propagation of Error Into Regions of Smoothness for Non-Linear Approximations to Hyperbolic Equations," *Comp. Meth. Appl. Mech. Eng.* **80**, 59–64 (1990).

Drikakis, D., "Embedded turbulence model in numerical methods for hyperbolic conservation laws," *Int. J. Num. Meth. Fluids* **39**, 763–781 (2002).

Drikakis, D., "Advances in turbulent flow computations using high-resolution methods," *Prog. Aero. Sci.* **39**, 405–424 (2003).

Ducros, F., Ferrand, V., Nicoud, F., Weber, C., Darracq, D., Gacherieu, C., and Poinsot, T., "Large-Eddy Simulation of the Shock/Turbulence Interaction," *J. Comp. Phys.* **152**, 517–549 (1999).

Engquist, B., Lötstedt, P., and Sjögreen, B., "Nonlinear Filters for Efficient Shock Computation," *Math. Comp.* **52**, 509–537 (1989).

Engquist, B., and Sjögreen, B., "The Convergence Rate of Finite Difference Schemes in the Presence of Shocks," *SIAM J. Num. Anal.* **35**, 2464–2485 (1998).

Garnier, E., Mossi, M., Sagaut, P., Comte, P., and Deville, M., "On the Use of Shock-Capturing Schemes for Large-Eddy Simulation," *J. Comp. Phys.* **153**, 273–311 (1999).

Garnier, E., Sagaut, P., and Deville, M., "Large Eddy simulation of shock/homogeneous turbulence interaction," *Comp. and Fluids* **31**, 245–268 (2002a).

Garnier, E., Sagaut, P., and Deville, M., "Large Eddy Simulation of Shock/Boundary-Layer Interaction," *AIAA J.* **40**, 1935–1944 (2002b).

Gottlieb, D., and Hesthaven, J. S., "Spectral methods for hyperbolic problems," *J. Comp. Appl. Math.* **128**, 83–131 (2001).

Grinstein, F. F., Fureby, C., and DeVore, C. R., "On MILES based on flux-limiting algorithms," *Int. J. Num. Meth. Fluids* **47**, 1043–1051 (2005).

Hill, D. J., and Pullin, D. I., "Hybrid tuned center-difference-WENO method for large eddy simulations in the presence of strong shocks," *J. Comp. Phys.* **194**, 435–450 (2004).

Koochesfahani, M. M., and Dimotakis, P. E., "Mixing and chemical reactions in a turbulent liquid mixing layer," *J. Fluid Mech.* **170**, 83–112 (1986).

Kreiss, G., Efraimsson, G., and Nordström, J., "Elimination of First Order Errors in Shock Calculations," *SIAM J. Num. Anal.* **38**, 1986–1998 (2001).

Laney, C. B., *Computational Gasdynamics*, (Cambridge University Press, Cambridge, UK, 1998).

LeVeque, R. J., *Finite Volume Methods for Hyperbolic Problems*, (Cambridge University Press, Cambridge, UK, 2002).

Lomov, I. N., Pember, R. B., Greenough, J. A., and Liu, B. T., "Patch-Based Adaptive Mesh Refinement for Multimaterial Hydrodynamics," Proceedings of the Five-Laboratory Conference on Computational Mathematics, Vienna, Austria, 19– 23 June 2005 (2005).

Majda, A., McDonough, J., and Osher, S., "The Fourier Method for Nonsmooth Initial Data," *Math. Comp.* **30**, 1041–1081 (1978).

Majda, A., and Osher, S., "Propagation of Error into Regions of Smoothness for Accurate Difference Approximations to Hyperbolic Equations," *Comm. Pure Appl. Math.* **30**, 671–705 (1977).

Margolin, L. G., and Rider, W. J., "A rationale for implicit turbulence modeling," *Int. J. Num. Meth. Fluids* **39**, 821–841 (2002).

Margolin, L. G., and Rider, W. J., "The design and construction of implicit LES methods," *Int. J. Num. Meth. Fluids* **47**, 1173–1179 (2005).

Mock, M. S., and Lax, P. D., "The Computation of Discontinuous Solutions of Linear Hyperbolic Equations," *Comm. Pure Appl. Math.* **30**, 423–430 (1978).

Orszag, S. A., and Jayne, L. W., "Local Errors of Difference Approximations to Hyperbolic Equations," *J. Comp. Phys.* **14**, 93–103 (1974).

Pirozzoli, S., "Conservative Hybrid Compact-WENO Schemes for Shock-Turbulence Interaction," *J. Comp. Phys.* **178**, 81–117 (2002).

Ponziani, D., Pirrozoli, S., and Grasso, F., "Development of optimized weighted-ENO schemes for multiscale compressible flows," *Int. J. Num. Meth. Fluids* **42**, 953–977 (2003).

Pope, S. B., *Turbulent Flows*, (Cambridge University Press, Cambridge, UK, 2000).

Ren, Y.-X., Liu, M., and Zhang, H., "A characteristic-wise hybrid compact-WENO scheme for solving hyperbolic conservation laws," *J. Comp. Phys.* **192**, 365–386 (2003).

Sagaut, P., *Large Eddy Simulation for Incompressible Flows: An Introduction*, second edition, (Springer-Verlag, New York, 2002).

Schilling, O., and Latini, M., *Weighted essentially non-oscillatory simulations and modeling of Complex Hydrodynamic Flows. Part 1. Regular Shock Refraction*, Lawrence Livermore Scientific Laboratory, Livermore, CA, UCRL-TR-205132 (2004).

Schilling, O., and Latini, M., *Weighted essentially non-oscillatory simulations and modeling of Complex Hydrodynamic Flows. Part 2. Single-Mode Richtmyer-Meshkov Instability with Reshock*, Lawrence Livermore Scientific Laboratory, Livermore, CA, UCRL-TR-212120 (2005a).

Schilling, O., and Latini, M., *Weighted essentially non-oscillatory simulations and modeling of Complex Hydrodynamic Flows. Part 4. Multi-Mode Richtmyer-Meshkov Instability with Reshock*, Lawrence Livermore Scientific Laboratory, Livermore, CA, in preparation (2005b).

Sengupta, T. K., Ganerwal, G., and Dipankar, A., "High Accuracy Compact Schemes and Gibbs' Phenomenon," *J. Sci. Comp.* **21**, 253–268 (2004).

Sengupta, T. K., Jain, R., and Dipankar, A., "A new flux-vector splitting compact finite volume scheme," *J. Comp. Phys.* **207**, 261–281 (2005).

Siklosi, M., and Kreiss, G., "Elimination of First Order Errors in Time Dependent Shock Calculations," *SIAM J. Num. Anal.* **41**, 2131–2148 (2003).

Stolz, S., and Adams, N. A. "Large-eddy simulation of high-Reynolds-number supersonic boundary layers using the approximate deconvolution model and a rescaling and recycling technique," *Phys. Fluids* **15**, 2398–2412 (2003).

Vandeven, H., "Family of Spectral Filters for Discontinuous Problems," *J. Sci. Comp.* **6**, 159–192 (1991).

Vetter, M., and Sturtevant, B., "Experiments on the Richtmyer-Meshkov Instability of an Air/SF_6 Interface," *Shock Waves* **4**, 247–252 (1995).

Wang, Z., and Huang, G. P., "An Essentially Nonoscillatory High-Order Padé-Type (ENO-Padé) Scheme," *J. Comp. Phys.* **177**, 37–58 (2002).